



Thomas Jefferson University
Jefferson Digital Commons

Department of Neurology Faculty Papers

Department of Neurology

11-1-2020

Contribution of left supramarginal and angular gyri to episodic memory encoding: An intracranial EEG study.


Daniel Y. Rubinstein
Thomas Jefferson University

Liliana Camarillo-Rodriguez
Thomas Jefferson University

Mijail D. Serruya
Thomas Jefferson University

Nora A. Herweg
University of Pennsylvania

Zachary J. Waldman
Follow this and additional works at: <https://jdc.jefferson.edu/neurologyfp>
Thomas Jefferson University

 Part of the [Neurology Commons](#)

[Let us know how access to this document benefits you](#)

See next page for additional authors

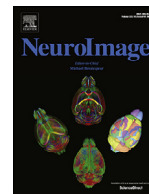
Recommended Citation

Rubinstein, Daniel Y.; Camarillo-Rodriguez, Liliana; Serruya, Mijail D.; Herweg, Nora A.; Waldman, Zachary J.; Wanda, Paul A.; Sharan, Ashwini D.; Weiss, Shennan A.; and Sperling, Michael R., "Contribution of left supramarginal and angular gyri to episodic memory encoding: An intracranial EEG study." (2020). *Department of Neurology Faculty Papers*. Paper 227. <https://jdc.jefferson.edu/neurologyfp/227>

This Article is brought to you for free and open access by the Jefferson Digital Commons. The Jefferson Digital Commons is a service of Thomas Jefferson University's [Center for Teaching and Learning \(CTL\)](#). The Commons is a showcase for Jefferson books and journals, peer-reviewed scholarly publications, unique historical collections from the University archives, and teaching tools. The Jefferson Digital Commons allows researchers and interested readers anywhere in the world to learn about and keep up to date with Jefferson scholarship. This article has been accepted for inclusion in Department of Neurology Faculty Papers by an authorized administrator of the Jefferson Digital Commons. For more information, please contact: JeffersonDigitalCommons@jefferson.edu.

Authors

Daniel Y. Rubinstein, Liliana Camarillo-Rodriguez, Mijail D. Serruya, Nora A. Herweg, Zachary J. Waldman, Paul A. Wanda, Ashwini D. Sharan, Shennan A. Weiss, and Michael R. Sperling



Contribution of left supramarginal and angular gyri to episodic memory encoding: An intracranial EEG study

Daniel Y. Rubinstein^{a,*}, Liliana Camarillo-Rodriguez^a, Mijail D. Serruya^b, Nora A. Herweg^c, Zachary J. Waldman^a, Paul A. Wanda^c, Ashwini D. Sharan^d, Shennan A. Weiss^{e,f,g,1}, Michael R. Sperling^{a,1}

^a Jefferson Comprehensive Epilepsy Center, Department of Neurology, Thomas Jefferson University, Philadelphia, PA, United States

^b Department of Neurology, Thomas Jefferson University, Philadelphia, PA, United States

^c Department of Psychology, University of Pennsylvania, Philadelphia, PA, United States

^d Department of Neurological Surgery, Thomas Jefferson University, Philadelphia, PA, United States

^e Department of Neurology, State University of New York Downstate Medical Center, Brooklyn, NY, United States

^f Department of Physiology and Pharmacology, State University of New York Downstate Medical Center, Brooklyn, NY, United States

^g Department of Neurology, New York City Health + Hospitals/Kings County, Brooklyn, NY, United States

ARTICLE INFO

Keywords:

Episodic memory
Ventral parietal cortex
Subsequent memory effect
Spectral tilt
iEEG

ABSTRACT

The role of the left ventral lateral parietal cortex (VPC) in episodic memory is hypothesized to include bottom-up attentional orienting to recalled items, according to the dual-attention model (Cabeza et al., 2008). However, its role in memory encoding could be further clarified, with studies showing both positive and negative subsequent memory effects (SMEs). Furthermore, few studies have compared the relative contributions of sub-regions in this functionally heterogeneous area, specifically the anterior VPC (supramarginal gyrus/BA40) and the posterior VPC (angular gyrus/BA39), on a within-subject basis. To elucidate the role of the VPC in episodic encoding, we compared SMEs in the intracranial EEG across multiple frequency bands in the supramarginal gyrus (SmG) and angular gyrus (AnG), as twenty-four epilepsy patients with indwelling electrodes performed a free recall task. We found a significant SME of decreased theta power and increased high gamma power in the VPC overall, and specifically in the SmG. Furthermore, SmG exhibited significantly greater spectral tilt SME from 0.5 to 1.6 s post-stimulus, in which power spectra slope differences between recalled and unrecalled words were greater than in the AnG ($p = 0.04$). These results affirm the contribution of VPC to episodic memory encoding, and suggest an anterior-posterior dissociation within VPC with respect to its electrophysiological underpinnings.

1. Introduction

The ventral parietal cortex (VPC) is well recognized to be involved in episodic memory, in addition to the classically associated functions of spatial cognition and attention (Sestieri et al., 2017; Berryhill et al., 2007). While individuals with lesions in the VPC do not exhibit gross memory deficits, and performance on cued recall is normal, performance on free recall is characterized by reduced detail (Berryhill et al., 2007). Imaging studies have similarly found that activation of the VPC (specifically in the angular gyrus) during encoding relates to subsequent confidence in memory retrieval, both at the level of fMRI BOLD networks (Gilmore et al., 2015) and single neurons (Rutishauser et al., 2018).

Disruption of the angular gyrus has also been found to affect memory confidence, without altering memory accuracy (Koen et al., 2018). In addition to subjective feelings of memory quality, other studies have found memory success to relate to VPC activation (Dickerson et al., 2007; Heinze et al., 2006; Uncapher and Wagner, 2009; Gilmore et al., 2015). For example, in a free recall task of visual images, Dickerson et al. found that fMRI activation of the left posterior VPC during encoding was significantly greater for subsequently recalled images than unrecalled (Dickerson et al., 2007). Similarly, another fMRI study found greater activation of left anterior VPC during encoding of subsequently freely recalled visually displayed words, especially in high performers (Heinze et al., 2006). The range of memory-related functions ascribed to the VPC, as well as the possibility for significant sub-regional variation

Abbreviations: AnG, angular gyrus; DMN, default mode network; LFA, low frequency activity; HFA, high frequency activity; SME, subsequent memory effect; SmG, supramarginal gyrus; VAN, ventral attention network; VPC, ventral parietal cortex.

* Corresponding author.

E-mail address: daniel.rubinstein@jefferson.edu (D.Y. Rubinstein).

¹ These authors share senior authorship.

<https://doi.org/10.1016/j.neuroimage.2020.117514>

Received 4 May 2020; Received in revised form 28 September 2020; Accepted 24 October 2020

Available online 1 November 2020

1053-8119/© 2020 The Authors. Published by Elsevier Inc. This is an open access article under the CC BY-NC-ND license (<http://creativecommons.org/licenses/by-nc-nd/4.0/>)

(Uncapher and Wagner, 2009), suggests that more can be learned about the contribution of the VPC to episodic memory encoding.

One dimension of VPC activity during encoding relates to the direction of the subsequent memory effect (SME), which refers to the difference in neural activation during encoding between items that are later recalled and those that are not recalled. Many studies have shown that increased fMRI BOLD activation in the VPC and its related networks during encoding predicts future recall failure (i.e., negative SME) (Uncapher and Wagner, 2009; Kim, 2011; Gilmore et al., 2015), however, these negative SME studies have mostly utilized recognition memory paradigms as opposed to free recall paradigms. This difference may be crucial, as recognition memory relies on different circuitry compared to free recall (Staresina and Davachi, 2006) and success in these different types of tests may reflect different encoding processes (Rugg et al., 2008; Hanslmayr and Staudigl, 2014). Indeed, in free recall, there is evidence for positive SMEs, i.e. increased activation in VPC during encoding of later-remembered items. While in fMRI this manifests as increased BOLD activation (Staresina and Davachi, 2006; Heinze et al., 2006; Dickerson et al., 2007), activation of the VPC in intracranial EEG (iEEG) studies manifests as concurrent decreased low-frequency and increased high-frequency power (Burke et al., 2014), a phenomenon documented as “spectral tilt” (Ezzayat et al., 2017).

An additional relevant dimension to the role of the VPC in episodic memory is its sub-regional heterogeneity. In the context of the attention-to-memory model (Cabeza et al., 2008), the VPC is distinguished from the dorsal parietal cortex, which is hypothesized to direct top-down goal-driven attention, in contrast to the bottom-up sensory-driven processing controlled by the VPC. The VPC itself may be divided into its anterior and posterior part, which respectively consist of the supramarginal gyrus (SmG)/BA40, and the angular gyrus (AnG)/BA39. The SmG of the anterior VPC has been hypothesized to mediate attention to external stimuli, while the AnG of the posterior VPC has been hypothesized to mediate attention to internal stimuli (Corbetta and Shulman, 2002; Cabeza et al., 2008; Buckner et al., 2008; Daselaar et al., 2013). This hypothetical distinction is further supported by their respective belonging to different networks, namely the SmG to the ventral attention network (VAN) and the AnG to the default mode network (DMN) (Yeo et al., 2011). How this distinction plays out during encoding though, remains an open question and the focus of our study.

To shed further light on the specific electrophysiology of the VPC during encoding and the potentially different roles of the SmG and AnG during encoding, we utilized iEEG recordings from patients with epilepsy performing a free recall task. Due to the verbal nature of the task and the preponderance of memory-related VPC findings in the left hemisphere compared to right hemisphere (Vilberg and Rugg, 2008), we focused on the left VPC. We specifically compared SMEs in the left SmG and left AnG within individual patients. In the VPC overall, we predicted a positive SME, characterized by increased spectral tilt, or increased high frequency and decreased low frequency spectral power. While we did not explicitly test externally-versus-internally oriented attention, we hypothesized that if the SmG mediates externally-oriented attention (Cabeza et al., 2008), then its activation would promote subsequent retrieval. We thus predicted more positive SMEs in the SmG compared to the AnG. Conversely, we speculated that if the AnG mediates internally-oriented attention, then the conflicting demands of contextual binding and suppression of internal attention might result in weakly negative SMEs in this region.

2. Methods

2.1. Patients

For this study we utilized a dataset of 274 patients with medication-resistant epilepsy enrolled in the Defense Advanced Research Projects Agency (DARPA) Restoring Active Memory (RAM) project who provided informed consent. Data were collected at 8 participating hos-

pitals, and the protocol was approved by their Institutional Review Boards, of: Columbia University Hospital (New York, NY), Dartmouth-Hitchcock Medical Center (Lebanon, NH), Emory University Hospital (Atlanta, GA), Hospital of the University of Pennsylvania (Philadelphia, PA), Mayo Clinic (Rochester, MN), National Institutes of Health (Bethesda, MD), Thomas Jefferson University Hospital (Philadelphia, PA), and University of Texas Southwestern Medical Center (Dallas, TX). Patients underwent surgery for implantation of subdural and depth electrode recording contacts, which were placed in order to identify and exclude epileptic areas (seizure onset and irritative zones). Patients were monitored for epileptic activity over the course of their hospital stay, during which they also performed a variety of cognitive tasks.

2.2. Behavioral task

Patients completed a verbal free recall task of randomly selected words from a list of commonly used nouns (<http://memory.psych.upenn.edu/WordPools>) used previously (Solomon et al., 2019). Patients viewed up to twenty-five twelve-word lists in an experimental session. The words in each session were drawn from the same 300-word pool, in different random orders. In each list, words were displayed sequentially over 30 s, with each word on screen for 1.6 s, and an inter-stimulus interval of 0.75–1 s. Patients were instructed to visualize each word as vividly as possible, and to focus only on the word being presented, and not on other words in the list. Word list presentation was followed by a 20 s arithmetic distractor task, in which patients completed simple addition problems. Patients were then given 30 s to recall as many words as possible (Fig. 1a). This block of encoding-distractor-recall epochs was repeated at most 25 times per session. Patients completed as many sessions as comfort allowed.

2.3. Intracranial EEG recordings

Intracranial recordings included those from depth, strip, and grid electrodes (AdTech Inc., PMT Inc.), which were implanted based on patient-specific needs and selection by clinical teams at each hospital. Recordings were collected with Nihon-Kohden EEG-1200, Natus XLTek EMU 128, or Grass Aura-LTM64 systems, depending on the site of data collection. Sampling rates ranged from 500 to 2000 Hz depending on site. During recording, data were referenced to common intracranial, scalp, or mastoid contacts. Electrodes were excluded from analyses if they were located in the seizure onset zone or displayed spikes, as assessed by clinical neurophysiologists. Data were referenced using a bipolar referencing scheme; the resulting bipolar virtual contacts are here referred to as “contacts”. These bipolar contacts were constructed from the difference signals of spatially adjacent electrodes. Grid electrodes were considered to have at most 4 (excluding diagonal adjacencies) adjacent contacts, with which to pair for a bipolar contact. To be precise, this leads to $N - 1$ bipolar contacts for depth and strip arrays of length N , and $M \times (2N - 1) - N$ contacts for grid contact arrays of length N and width M electrodes.

2.4. Electrode localization

Prior to electrode implantation, T1- and T2-weighted MRIs were obtained for each patient. FreeSurfer (<http://surfer.nmr.mgh.harvard.edu/>) was used to construct individual subject brain surfaces and cortical parcellations according to the Desikan–Killiany atlas (Desikan et al., 2006), based on the T1-weighted MRIs. Post-implantation CT scans were then co-registered with the pre-implantation MRIs using Advanced Neuroimaging Tools (ANTs) (Avants et al., 2008) with neuroradiologist supervision, to enable regional localization of electrode contacts within the Desikan–Killiany atlas. An in-house pipeline (https://github.com/pennmem/neurorad_pipeline) was used to transform individual-space coordinates into average FreeSurfer space (defined by the fsaverage

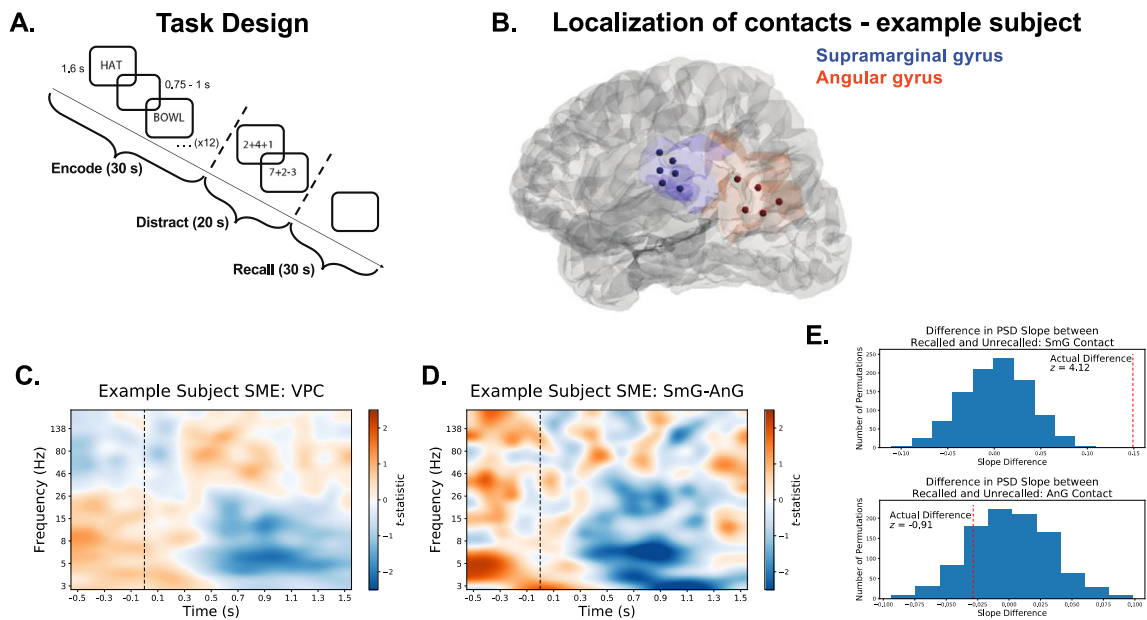


Fig. 1. Overview of study design. A) Illustration of free recall verbal episodic memory task. For each list, words were displayed on screen for 1.6 s each with jittered inter-stimulus intervals between 0.75 and 1 s, followed by a 20 s arithmetic distractor task, ending with a 30 s window to recall as many words as possible. B) Localization of electrode contacts in regions of interest (blue: supramarginal gyrus [SmG]; orange: angular gyrus [AnG]) for an example subject. C) Subsequent memory effect (SME) averaged over all contacts in ventral parietal cortex (VPC) of a single representative subject. Orange indicates greater power during encoding of words that were later recalled compared to unrecalled; blue indicates less power. Word onset is at 0 ms. D) Difference in SME at each time-frequency bin between sub-regions of ventral parietal cortex in the same subject as shown in (C). Orange indicates more positive SME in the supramarginal gyrus (SmG) compared to angular gyrus (AnG), and blue indicates more negative SME in SmG. Note the similarity to the overall VPC plot (C). Time-frequency plots are smoothed for visualization. E) Histograms showing z -score of tilt SME for example contacts in SmG (top) and AnG (bottom), based on tilt differences between recalled and unrecalled trials, and a null distribution constructed from randomly permuting recalled word labels.

brain) for each electrode contact, utilizing previously published methods (Groppe et al., 2017). Finally, locations for strip and grid contacts were projected to the cortical surface to correct for post-operative brain shift (Dykstra et al., 2012). This procedure was performed for contacts in both the individual FreeSurfer space as well as the average FreeSurfer space. Only electrode contacts within the left “supramarginal” or left “inferior parietal” (i.e., AnG) regions were used in the present analysis. To perform group-level analyses of contact locations, we used coordinates in average FreeSurfer space. Otherwise, we used coordinates in individual FreeSurfer space. Visual representations of contact localizations were generated using BrainNet Viewer (Xia et al., 2013, <http://www.nitrc.org/projects/bnv/>).

2.5. Electrode and patient selection

Of the 274 patients in the initial pool, patients were included in subsequent analyses only if they had at least 2 physical electrode contacts (resulting in at least 1 bipolar depth or surface contact) within both the left SmG, and left AnG, as defined in individual space (see Fig. 1b, S3 for examples). Electrode contacts that were located in the seizure onset or irritative zone were excluded. Twenty-five patients met this criteria, and comprised the initial analysis set.

2.6. Spectral power analysis

Our analysis focused on the electrophysiological power during the 1.6 s encoding period, during which the word was displayed. We used MNE-Python (Gramfort et al., 2013) to divide the data into epochs including a 1 s buffer period on either side of the encoding period, resulting in epochs from 1 s prior, to 2.6 s following word presentations. The data were then notch filtered, using a 4 Hz width filter, at 60 Hz, 120 Hz, and 180 Hz to reduce power line noise. Using Morlet wavelets

(number of cycles = 6), we then extracted power at 24 log-spaced frequencies from 3 to 200 Hz and removed the buffer period. Power values were log-transformed (base 10) and averaged over 16 non-overlapping 100 ms time bins for each frequency. We then z -scored the resulting power values on a session-by-session basis, by subtracting the mean and standard deviation of 500 ms pre-stimulus power on a frequency-wise basis. We further excluded the first 200 ms following word presentation, resulting finally in a 0.2–1.6 s epoch of interest, a time period previously used in analyses of this task (Manning et al., 2012).

2.7. Subsequent memory effect

We tested for subsequent memory effects (SME) by using independent t -tests to compare power during subsequently recalled, to unrecalled words. This SME was computed independently for each bipolar contact, for each frequency and time bin, to produce a time-frequency map of t -statistics. The resulting t -statistics were then averaged over contacts to produce one time-frequency map for the VPC overall, one for the SmG, and one for the AnG, for each patient. Computing t -statistics on a per-contact basis and then averaging the statistics over contacts, helps to mitigate the potential effect of varying numbers of contacts in each patient. Finally, these individual patient-level time-frequency maps were aggregated in group-level statistical analyses, in which false discovery rate (FDR) (Benjamini-Hochberg, 1995) was used to adjust p -values for multiple comparisons. For statistical tests that were performed on a time-frequency-wise basis, FDR (Benjamini-Hochberg)-adjusted p -values were computed to account for multiple comparisons.

2.8. Spectral tilt

To compute the spectral tilt between recalled and unrecalled trials for a given subject and contact, we computed the average power spectrum for all recalled, and unrecalled trials separately, using the MNE-

Table 1
Behavioral summary.

	Mean (SD)	Range
Number of sessions	2.1 (0.9)	1–4
Lists per session	19.3 (5.7)	8–25
Recall performance	24.0% (11.5)	8.8–53.9%
Math distractor performance	91.8% (8.7)	65.0–100%

Python (Gramfort et al., 2013) implementation of Welch’s method. We then log-transformed the power spectrum, calculated a linear fit of the log-transformed power spectra using linear regression, and subtracted the slopes of the recalled and unrecalled fits. A null distribution of slope differences was constructed by randomly permuting the recalled and unrecalled trials 1000 times. Finally, the real difference between the recalled and unrecalled slopes was converted into a z -score using this null distribution (see Fig. 1e for example). The z -scores were averaged across contacts in a given region, for each subject, except when implementing linear mixed effects (LME) models, where the z -scores of each individual contact were used. To test the effects of serial position on spectral tilt we followed prior work that has reported differences in spectral power based on serial position (Serruya et al., 2014), and calculated spectral tilt for early (serial positions 1–4), middle (positions 5–8), and late (positions 9–12), which we coded as 1, 2, and 3, respectively, in the model. The LME model was implemented in Python version 3.7.7, using the “statsmodels” package version 0.10.0 (Lindstrom and Bates, 1988; Seabold and Perktold, 2010). Model comparisons were performed using likelihood ratio tests.

2.9. Functional heterogeneity

To test for differences in functional heterogeneity between the SmG and AnG we compared proportions of positive and negative SMEs between the SmG and AnG using Fisher’s exact test. This was performed including all SMEs, as well as only SMEs that were significant ($|z| > 1.96$).

To test for anatomical clustering of positive and negative SMEs, we computed the centroids of the contacts that showed positive SMEs and those that showed negative SMEs, and computed the Euclidean distance between these two centroids. We then performed a permutation test where the SME values of all contacts were randomly shuffled, and the distance between the positive SME centroid and negative SME centroid was recomputed. This procedure was performed 10,000 times to generate a null distribution of centroid distances. The real distance between the two centroids was thus converted into a z -score.

3. Results

3.1. Behavioral results

Among the initial subset of 25 patients, math distractor performance was 0% for one patient, who was therefore excluded from all analyses. The remaining 24 patients represent the main analysis set. Behavioral performance measures are listed in Table 1. Serial position effects on recall performance were observed, in particular a primacy effect wherein items displayed earlier in the encoding list were recalled with greater probability (Fig. S1).

To assess the possibility of practice effects of familiarity with the same words being presented across sessions, we examined the difference in performance between the first and last sessions performed by patients who completed more than one session. The difference in performance was not significantly different than 0 ($M = -0.9\%$; $t(23) = -0.45$, $p = 0.66$).

Among these 24 patients, there totaled 303 bipolar contacts in the left VPC: 172 in the SmG, and 131 in the AnG after excluding contacts in the SOZ or irritative zone (39 in the SmG and 33 in the AnG). The

average number of contacts in the left VPC per patient was 12.6 ± 5 (in SmG: 7.2, range: 3–14; in AnG: 5.5, range: 1–14). All but two patients were right-handed; results did not change substantially upon excluding these two patients.

3.2. VPC subsequent memory effect: increased spectral tilt

We first asked whether there were SMEs over the spectral range in the VPC overall (see Fig. 1c for example subject). We observed significant SMEs in theta and high gamma ranges in the VPC (Fig. 2a). Negative SMEs (reduced power for words that were subsequently recalled) predominated in frequencies below the gamma range, and peaked at 4 Hz at 1.5 s ($M = -0.56$; $t(23) = 5.55$, FDR-adjusted $p = 0.002$). Positive SMEs (increased power for later-recalled words) predominated in gamma frequencies and above, peaking at 116 Hz at 0.7 s ($M = 0.25$; $t(23) = 4.38$, FDR-adjusted $p = 0.003$).

The observed broad-band effect, with negative SMEs in lower frequencies and positive SMEs in higher frequencies, has been well-replicated in memory studies (Burke et al., 2014; Greenberg et al., 2015). The pattern can be conceptualized as a “spectral tilt” (Ezzyat et al., 2017), and has been related to general neural activation measures such as neural firing and BOLD activity (Burke et al., 2015; Winawer et al., 2013). Here, the power spectrum during encoding of later-recalled words is tilted relative to the power spectrum during unrecalled words, usually with ~ 30 Hz as the ‘fulcrum’ of this tilt. This phenomenon is reflected in Fig. 2a, as a stark line at ~ 30 Hz separating positive SMEs from negative SMEs. Based on the observation of significant power modulations starting ~ 0.5 s post stimulus (Fig. 2a), we specifically compared the spectral tilt between recalled and unrecalled words from 0.5 to 1.6 s post stimulus, and found significantly increased tilt ($t(23) = 3.54$; $p = 0.0017$). As illustrated in Figs. 1d and 2b, a positive tilt corresponds to reduced low-frequency power (negative SMEs) and increased high-frequency power (positive SMEs) during subsequently recalled words.

3.3. Sub-regional analysis: SmG vs. AnG

Having established a robust subsequent memory effect in VPC, we asked if there was a difference in the spectral tilt SME between the SmG and AnG. A paired t -test revealed significantly greater tilt in the SmG ($M = 0.52$; $SD = 0.13$) compared to the AnG ($M = 0.12$; $SD = 0.17$) ($t(23) = 2.17$, $p = 0.040$; Fig. 3b). The more positive tilt SME in the SmG indicates greater difference in slopes between power spectra of recalled and unrecalled words. This is also reflected in the greater negative SMEs at lower frequencies and greater positive SMEs at higher frequencies (Fig. 3a). We additionally asked if the AnG exhibited reduced SMEs partly due to a greater number of negative SMEs. We therefore compared the proportions of contacts with positive and negative SMEs in each region, over all subjects and contacts combined. Contacts in the AnG were significantly more likely to be negative, compared to the SmG (Fisher’s exact test, $p = 0.048$) with 48/172 (27.9%) of contacts in the SmG being negative, and 51/131 (38.9%) of contacts in the AnG being negative. Among contacts showing significant SMEs ($|z| > 1.96$), 3/17 (17.6%) in the SmG were negative, and 3/6 (50%) in the AnG were negative. However, this difference was not statistically significant (Fisher’s exact test, $p = 0.28$).

Given previous reports of the effect of serial position on HFA and LFA (Serruya et al., 2014), we used a linear mixed effects model to test whether the spectral tilt SME was related to serial position (defined by early, middle, or late serial positions). We first modeled the SME with a fixed effect of region and random effect (intercept) of subject. In this model there was a significant effect of region ($p = 0.005$; Table S1), whereby the SmG exhibited greater spectral tilt SME. We then implemented a model with fixed effects of region, serial position, and their interaction, and the same random effect of subject as the first

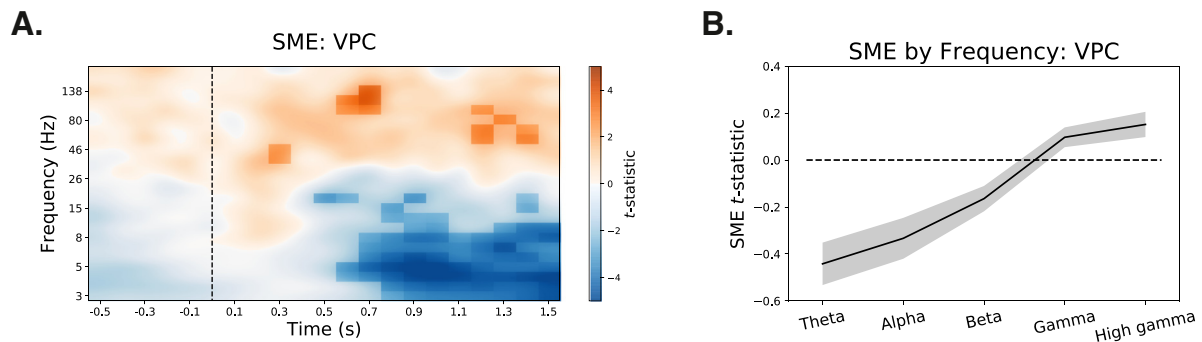


Fig. 2. Subsequent memory effects in VPC. A) Time-frequency representation of significant subsequent memory effects across subjects in all VPC contacts, blue showing negative SMEs and orange showing positive SMEs. Time-frequency bins with FDR-adjusted $p < 0.05$ are highlighted with rectangular overlays. Word is displayed from 0 to 1.6 s. B) Illustration of overall spectral tilt of SME in VPC, from 0.5 to 1.6 s, showing greater negative SME in lower frequencies and greater positive SME in higher frequencies. Shaded region indicates ± 1 SEM.

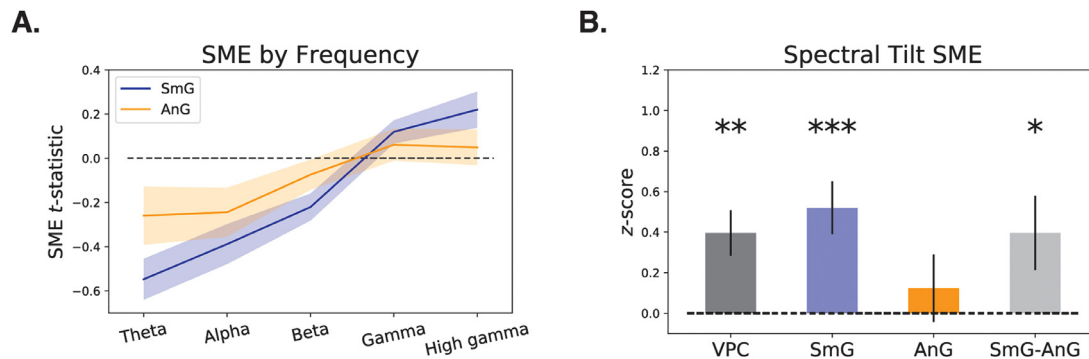


Fig. 3. Subsequent memory effects in SmG and AnG. A) Illustration of overall spectral tilt of SME in SmG (blue) and AnG (orange), showing greater negative SME in lower frequencies and greater positive SME in higher frequencies. Shaded region indicates ± 1 SEM. B) Spectral tilt SME over encoding time period from 0.5 to 1.6 s, in VPC (black), SmG (blue), AnG (orange), and difference (gray), illustrating the more negative SME at lower frequencies and more positive SME at higher frequencies in SmG compared to AnG. Error bars indicates ± 1 SEM. Asterisks indicate $p < 0.05$ (*) and $p < 0.001$ (**).

model. In this second model there was again a significant effect of region ($p = 0.029$; Table S1), whereas neither the effect of serial position nor the interaction of region serial position were significant ($p = 0.48$, $p = 0.25$ respectively). As the log likelihood of the simpler first model (-1127.5) was greater than for the second model (-1131.0), there was no evidence that including serial position as a predictor of SME improved the model. Taken together, this suggests that the spectral tilt SME in SmG was larger than in AnG regardless of serial position.

We then asked whether there was a difference at the individual time-frequency level between the two regions (see Fig. 1d for example subject). We statistically assessed this question at a within-subject level, with a paired t -test of the time-frequency maps from both regions (Fig. 5a). The difference between SmG and AnG followed a pattern similar to the VPC overall: greater negative SMEs in the SmG at lower frequencies, and greater positive SMEs in the SmG at higher frequencies. However, differences between SmG and AnG reached significance after FDR adjustment at only one isolated time-frequency bin: 19 Hz at 0.8 s ($M = -0.65$; $t(23) = -4.89$; FDR-adjusted $p = 0.02$).

We examined the time-frequency plots of SME for the SmG and AnG separately as well. In the SmG we observed significant SMEs (Fig. 5b) at similar times and frequencies to the VPC overall: the peak negative SME was observed at 5 Hz at 1.0 s ($M = -0.78$; $t(23) = -6.6$; FDR-adjusted $p = 0.0002$) and peak positive SME at 67 Hz at 1.3 s ($M = 0.40$; $t(23) = 3.67$; FDR-adjusted $p = 0.008$). However, SMEs were much weaker in the AnG (Fig. 5c), where we observed no time-frequency bins with $p < 0.05$ after adjusting for multiple comparisons. The peak negative SME in the AnG occurred at 9 Hz at 1 s ($M = -0.49$; $t(23) = -4.04$; FDR-adjusted $p = 0.3$), and the peak positive SME occurred at 39 Hz at 0.2 s ($M = 0.24$; $t(23) = 2.84$; FDR-adjusted $p = 0.3$).

Finally, we examined the anatomical clustering of positive and negative SMEs irrespective of regional localization. Across all subjects, the clusters of contacts showing positive and negative SMEs were largely overlapping (Fig. 4a,b), but were separated by a distance of 5.0 mm between the centroids of the two clusters (Fig. 4c). While small, this distance was statistically significant ($p = 0.017$; Fig. 4d), and was oriented such that positive SMEs were more anterior/dorsal, and negative SMEs were more posterior/ventral, consistent with the relative orientations of the SmG and AnG.

4. Discussion

Here we used a free recall paradigm to assess the electrophysiological underpinning of the VPC's role in episodic encoding. More specifically, this is the first study to test the differential contribution of its anterior and posterior sub-regions – the SmG and AnG. We found an SME in the VPC with decreased low frequency activity (LFA) (<30 Hz) and increased high frequency activity (HFA) (>30 Hz) in spectral power throughout the encoding epoch, which is consistent with previous iEEG reports using separate datasets (Burke et al., 2014). Moreover, this pattern of decreased LFA and increased HFA, or spectral tilt, was significantly greater in the SmG compared to the AnG.

4.1. VPC subsequent memory effect

The main finding of significant SME in the VPC replicates previous studies that demonstrate a role for this region in episodic memory encoding, and complements other studies that have demonstrated the VPC's role in retrieval (Wagner et al., 2005; Rugg and King, 2018). Using a

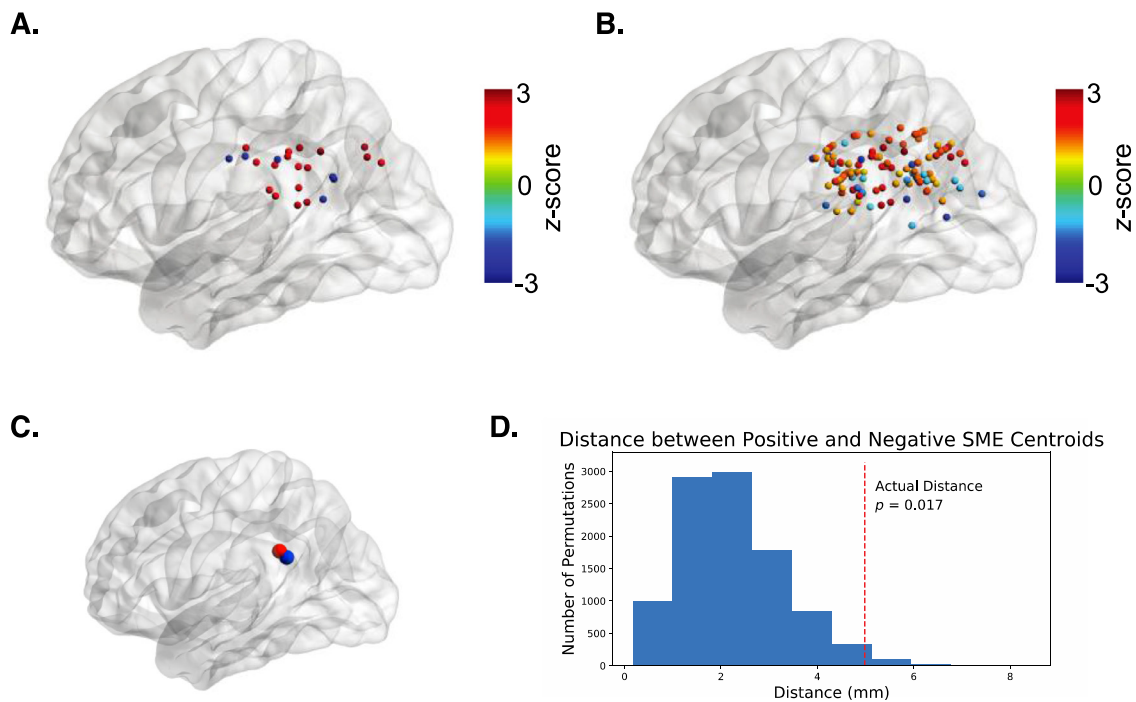


Fig. 4. Sub-regional heterogeneity of SMEs. A) Channels with significant SMEs ($|z| > 1.96$; left), or B) trending ($|z| > 1$; right) are plotted on an average brain. C) Centroids of all positive (blue) and negative (red) SMEs. D) Null distribution of centroid distances. Red dashed line indicates the actual distance between the two centroids.

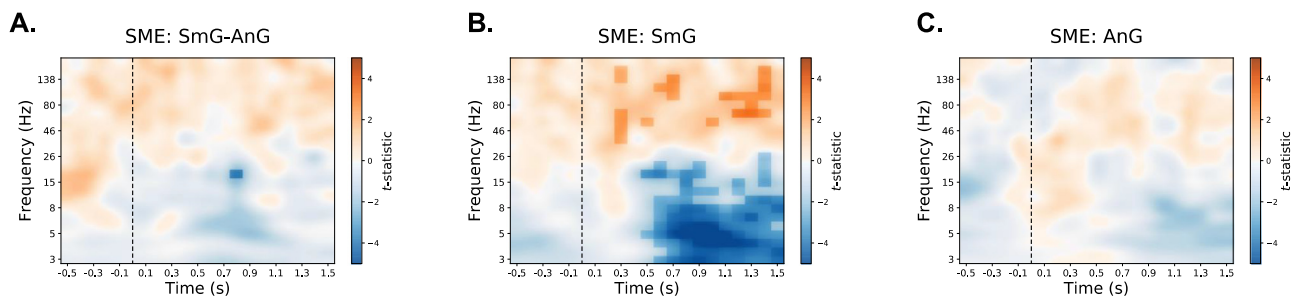


Fig. 5. Time-frequency comparison of subsequent memory effects. A) Time-frequency representation of difference in SME across subjects between SmG and AnG contacts, with blue showing more negative, and orange showing more positive SME in SmG compared to AnG. Time-frequency bins with FDR-adjusted $p < 0.05$ are highlighted with rectangular overlays. Word is displayed from 0 to 1.6 s. B, C) Time-frequency representation of SME across subjects in SmG (B) and AnG (C) contacts, with blue showing negative SMEs and orange showing positive SMEs. Note the significant time-frequency bins in the theta band (~ 5 Hz) at 1.0 s and high gamma band (~ 60 – 150 Hz) at 1.3 s, in the SmG (B). Vertical dashed lines indicate stimulus presentation at time 0.

verbal free recall task similar to ours, [Burke et al. \(2014\)](#) also found an SME of increased HFA in the left posterior parietal cortex during encoding. There, the temporal profile of the SME showed a peak around 1 s post-stimulus, and was relatively sustained compared to the highly peaked profile of other regions such as the visual and medial temporal cortices. This late-peaking sustained response supports the notion that the VPC mediates associative processes related to memory formation, possibly in addition to stimulus-specific information. While we did not test for stimulus-specific semantic information in our study, previous reports show category-specific information encoded by BOLD activation of the AnG ([Lee et al., 2017](#)), and semantic information is known to be processed by a widespread cortical network that includes the SmG and AnG ([Binder et al., 2009](#)).

4.2. Differential roles of SmG and AnG

The specific focus of our study addresses a more nuanced question of a potential anterior-posterior dissociation of function within the VPC. This fMRI-supported hypothesis posits that the SmG

processes external/perceptual information, whereas the AnG processes internal/conceptual information ([Corbetta and Shulman, 2002](#); [Buckner et al., 2008](#); [Cabeza et al., 2008](#); [Binder et al., 2009](#); [Daselaar et al., 2013](#)). This distinction is consistent with the difference in resting state networks to which each region belongs, namely the ventral attention network for the SmG, and the default mode network for the AnG ([Yeo et al., 2011](#); [Table 2](#)). Indeed, previous studies have hypothesized that the network associations of the AnG explain its predominantly negative SMEs ([Daselaar et al., 2004](#); [Shrager et al., 2008](#); for review, see [Kim, 2011](#)). Although it should also be noted that the AnG may belong to a “Parietal Memory Network” that is separate from the DMN ([Gilmore et al., 2015](#)). While fMRI studies may easily compare the SmG to AnG, to our knowledge this is the first within-subject iEEG comparison of these two regions during episodic encoding. We hypothesized that externally-oriented processing would be more advantageous for episodic encoding (conversely, evidence of VPC contribution to episodic retrieval has converged on the AnG, [Rugg and King, 2018](#)). Together, along with the tendency for BOLD activation to correlate with increased high frequency power ([Conner et al., 2011](#)), we predicted greater SME in the

Table 2
Neuroanatomy of supramarginal and angular gyri.

	Anterior VPC	Posterior VPC
Gyrus	Supramarginal gyrus (SmG)	Angular gyrus (AnG)
Brodmann area	BA40	BA39
Location	Ventral to intraparietal sulcus, anterior area around end of Sylvian fissure bordered anteriorly by postcentral sulcus, and ventrally by superior temporal gyrus. Includes temporoparietal junction.	Ventral to intraparietal sulcus, posterior to Sylvian fissure, bounded posteriorly by occipital cortex, and ventrally by lateral temporal gyri
Functional network	Ventral Attention Network (Yeo et al., 2011)	Default Mode Network (Yeo et al., 2011)
White matter connectivity	AnG, superior parietal lobule, and primary sensory cortices via local association fibers; middle and superior temporal gyri via arcuate fasciculus and middle longitudinal fasciculus; inferior and middle frontal gyri via superior longitudinal fasciculus (Burks et al., 2017)	SmG and superior parietal lobule via local association fibers; primary sensory cortices via superior longitudinal fasciculus; middle temporal gyrus via arcuate fasciculus; lateral occipital cortex via inferior longitudinal fasciculus (Burks et al., 2017)

SmG compared to the AnG. We confirmed this prediction: the spectral tilt SME, characterized by decreased LFA and increased HFA, was significantly greater in the SmG.

In addition to observing a difference in SMEs between the SmG and AnG, we also observed differences in anatomical locations of positive and negative SMEs regardless of region, whereby more anterior/dorsal contacts exhibited more positive SMEs compared to posterior/ventral contacts (Fig. 4d). This supports the notion of an anterior-posterior gradient of function within the VPC (Cabeza et al., 2008). Consistent with these prior hypotheses, we also found that contacts in the AnG were more likely to exhibit negative SMEs than those in the SmG. Together, these results are also consistent with prior fMRI studies showing that activation of the AnG during encoding is detrimental to future recall (Kim, 2011), and support our initial hypothesis of weakly negative SMEs in the AnG. In other words, successful encoding is supported not only by greater activation of the SmG compared to the AnG, but also by de-activation of parts of the AnG.

One natural question this raises is whether the two regions compete for cognitive and physiological resources. If it is behaviorally useful for them to exhibit complementary patterns of activation, it may be physiologically beneficial to share resources as well. While this idea is most likely an oversimplification, evidence from resting-state fMRI studies showing anti-correlations between anterior and posterior ventral parietal cortex, does support a competitive relationship to some extent (Buckner et al., 2008).

While our results are consistent with the hypothesis that the SmG mediates externally-oriented attention, and the AnG mediates internally-oriented attention, one may speculate a necessary balance between these two attentional processes, especially for free recall tests. Since free recall relies on internally-generated cues, the binding of external stimuli to internal context during encoding is necessary for successful recall (Staresina and Davachi, 2006; Lee et al., 2017). We hypothesize that without sufficient internally-oriented attention, this binding will not occur. Specifically, when one observes a new word during encoding, the SmG enhances attention to the external stimulus from 0 to 1 s post-stimulus, and then AnG activity highlights the internal context, and facilitates the binding of the incoming stimulus to the ongoing context representation. The balance between internal and external attention may manifest in the weakly positive SME observed in the AnG. We note, however, that this study was not designed to test the relative external-versus-internal allocation of attention, and we recognize the highly speculative nature of our interpretation of AnG activation patterns.

4.3. Positive vs. negative SME

The question of positive or negative SME has found discrepant answers in different studies. Large meta-analyses of fMRI studies have concluded that a negative SME predominates in the VPC (Uncapher and Wagner, 2009; Kim, 2011). However, when restricting to free recall as opposed to recognition paradigms, the majority of evidence points instead to positive BOLD SMEs (e.g. Staresina and Davachi, 2006; Heinze et al., 2006; Dickerson et al., 2007). As briefly discussed above,

we argue that since successful free recall relies solely on internal cues, it necessitates contextual binding between the (external) stimulus and internal associational structures. In contrast, recognition memory can take greater advantage of external cues and thus may rely on at least partially distinct encoding processes, including greater suppression of the DMN. Previous reports support such a relationship between retrieval tests and encoding processes (Rugg et al., 2008). While speculative, the negative SMEs observed in recognition tasks may thus reflect the decreased need for external-internal associations. For example, a recent fMRI study examining subsequent memory effects for free recall and recognition found that default network regions including the medial prefrontal, posterior cingulate, and right angular gyrus exhibited negative subsequent memory effects only for recognition tests, but not for free recall (Hill et al., 2020). Further evidence for the distinction between free recall and recognition tests was directly tested by Staresina and Davachi (2006), who combined a free recall and recognition paradigm: words (nouns) were presented visually on screen, but additionally included a color background, and subjects assessed the plausibility of the noun existing in that color. After a distractor period, a period of recall was provided before the subsequent recognition memory test. There they found that BOLD activation in the left SmG was specific to successful encoding of freely recalled items, and was not observed during encoding of correctly recognized items. Similarly, in a study by Dickerson et al. (2007), in which subjects were shown images of common objects and asked to recall them after a distractor period, a significant SME in left inferior parietal cortex was found. While there is not a direct correspondence between iEEG spectral power patterns and fMRI BOLD activation, the latter is generally associated with increased high frequency power. Thus, we conclude that our findings and those of Burke et al. (2014) support the positive SME shown by Staresina and Davachi (2006) and other select fMRI studies (Heinze et al., 2006; Dickerson et al., 2007).

However, some evidence also suggests a more nuanced landscape of cortical oscillatory contributions to memory. In a study combining EEG and fMRI, Hanslmayr et al. (2011) also used free recall to investigate SMEs in different frequency ranges across the brain and the potentially differential relationships between EEG and fMRI. While they also found that decreased beta (17–20 Hz) power predicted later remembering (albeit in inferior prefrontal regions), they found that increased theta in temporoparietal electrodes predicted recall. A direct comparison between our studies is difficult: there are likely differences in the signals detected from scalp EEG compared to iEEG, as well as in the analysis procedures (e.g. using bipolar referencing) that would specifically lead to observing increased theta in scalp EEG but not in iEEG (Herweg et al., 2020). Subtle differences in the task paradigm may also contribute in unknown ways (Hanslmayr et al., 2009). For example, Hanslmayr et al. (2011) utilized a directed forgetting paradigm in which subjects were instructed to only recall the second half of some lists. While this did not affect the fMRI results, other studies have demonstrated robust effects of list serial position on oscillatory power and SME (Serruya et al., 2014). More research is needed to clarify the effects of these and yet other task variations on SME.

4.4. Spectral tilt and oscillations

The electrophysiological differences between the two regions mirror the main effects, which can be summarized as a spectral “tilt” phenomenon (Ezzyat et al., 2017), with concurrently decreased LFA and increased HFA. While this spectral tilt is not specific to memory processing, and HFA especially is regarded as a general signal of cortical activation rather than being specific to memory formation (Crone et al., 2006), the same pattern of results has been found in other memory studies across much of the cortex (Burke et al., 2014; Ezzyat et al., 2017). In contrast to broad spectral changes, theta oscillations occupy a privileged position in models of memory function and contextual processing primarily in the medial temporal lobe (Solomon et al., 2019). Here we characterize our findings as a spectral tilt rather than decreased theta, due to the gradual nature of the SME changes from low to high frequency, and the stark distinction at ~30 Hz between negative and positive SME. Nevertheless, it is possible that in addition to spectral tilt-related processes, there is also a specific theta (or other) oscillatory component, especially considering that the strongest low-frequency component of the SME observed here occurred in the theta band (Fig. 2a). Indeed, previous evidence highlights the point that both phenomena contribute to this pattern, as individual frequency effects are dissociable in space and time, and sometimes by task condition (Fellner et al., 2019).

4.5. Limitations and future directions

One limitation of the present study relates to the variable placement of electrode contacts in the VPC, due to patients’ individual clinical demands. Relatedly, we here used an anatomically-based parcellation (Desikan-Killiany) for technical considerations and for ease of comparison with other studies. If there were a functional segregation of VPC finer than broadly distinguishing between the SmG and AnG, as might be inferred from cytoarchitectural and functional studies (Caspers et al., 2006; Igelström and Graziano, 2017), then those differences may affect our results in unknown ways. Specifically, the SmG and AnG are believed to be composed of 5 and 2 distinct sub-regions, respectively, which roughly progress from the anterior to posterior end of the VPC (Caspers et al., 2006). An examination of these more spatially-resolved, and functionally-defined differences in episodic processing might provide further insights. Furthermore, we did not establish the DMN or VAN in this study, so discussion of the SmG and AnG with respect to their putative network associations are somewhat speculative.

While previous studies have examined the effects of inhibitory electrical stimulation of the AnG on retrieval success (Sestieri et al., 2013), future studies may likewise utilize rTMS or other stimulation methods to more directly and causally probe the roles of these regions during encoding. We would predict that rTMS-mediated suppression of activity in the SmG would impair performance on memory tasks relying on externally-oriented attention, whereas suppression of activity in the AnG would impair memory relying on internally-oriented attention, for example when a greater degree of contextual binding is required. Interestingly, one study has tested the effect of TMS on left AnG during encoding of a paired associative memory task, finding that while memory accuracy was unaffected, memory confidence was adversely affected by TMS (Koen et al., 2018).

A further limitation of this study is the use of a bipolar referencing scheme, which may impact our ability to observe positive theta SME. As has been previously discussed (Herweg et al., 2020), positive theta SMEs may be obscured by the spatial filtering inherent in bipolar referencing. In this case, only the edges of the regions of interest would show the positive theta SME. Future studies could examine the impact of different referencing schemes on theta band SMEs, to confirm this hypothesis.

Finally, but importantly, the subjects of this analysis were patients with epilepsy, which may constrain the generalizability of the findings to healthy controls due to pathological activity or potential network reconfigurations. However, we note that previous studies have not found significant differences in neural SMEs between these two groups (Long et al., 2014; Hill et al., 2020).

5. Conclusions

To conclude, we provide evidence for distinct roles in episodic encoding in left SmG and AnG, as the anterior and posterior left VPC, respectively. Previous work has demonstrated a role for the VPC in episodic retrieval (Rugg and King, 2018) and encoding (Kim, 2011), with further suggestions that the SmG and AnG differ along the lines of externally-oriented and internally-oriented processing (Daselaar et al., 2013). This difference is also potentially reflected in the different networks to which each sub-region belongs, namely the VAN (for the SmG) and DMN (for the AnG). We further extend this hypothesis to episodic encoding. By directly comparing SmG and AnG, we show that the SmG has a preferential role in encoding, based in part on increased spectral tilt of reduced LFA and increased HFA.

Data and code availability

Data used in this project is available by request at http://memory.psych.upenn.edu/Request_RAM_Public_Data_access and analysis code is freely available at https://osf.io/yuc7x/?view_only=653e4e58ede848759e671b25036fc01f.

Declaration of Competing Interest

MRS is a consultant/advisor for Medtronic (fee to institution); is a consultant for NeurologyLive; received research support (to institution) from Eisai, Engage, Medtronic, Neurelis, Pfizer, SK Life Science, Inc., Takeda, UCB, and Xenon; and has been a speaker for Eisai.

CRediT authorship contribution statement

Daniel Y. Rubinstein: Conceptualization, Methodology, Software, Validation, Formal analysis, Writing - original draft. **Liliana Camarillo-Rodriguez:** Conceptualization, Investigation, Writing - review & editing. **Mijail D. Serruya:** Conceptualization, Writing - review & editing. **Nora A. Herweg:** Conceptualization, Writing - review & editing. **Zachary J. Waldman:** Conceptualization, Writing - review & editing. **Paul A. Wanda:** Software, Investigation, Writing - review & editing, Data curation, Project administration, Supervision. **Ashwini D. Sharan:** Investigation, Supervision. **Shennan A. Weiss:** Conceptualization, Resources, Writing - review & editing, Supervision. **Michael R. Sperling:** Conceptualization, Investigation, Resources, Writing - review & editing, Supervision, Funding acquisition.

Acknowledgments

This work was supported by Defense Advanced Research Projects Agency (DARPA) grant N66001-14-2-4032. DARPA had no involvement in study design, data collection, data analysis, data interpretation, report writing, or decision to submit for publication. We thank Ethan Solomon at the University of Pennsylvania for programming and analysis assistance. We also thank Pamela Walter and the Postdoc Scientific Editing and Reviewing Team at Thomas Jefferson University for valuable assistance in editing the manuscript. Most of all we thank the patients who generously devoted their time and energy to this research.

Ethics statement

All study participants provided written informed consent, with protocol approval granted by IRB #2 of University of Pennsylvania IRB.

Supplementary materials

Supplementary material associated with this article can be found, in the online version, at [doi:10.1016/j.neuroimage.2020.117514](https://doi.org/10.1016/j.neuroimage.2020.117514).

References

- Avants, B.B., Epstein, C.L., Grossman, M., Gee, J.C., 2008. Symmetric diffeomorphic image registration with cross-correlation: Evaluating automated labeling of elderly and neurodegenerative brain. *Medical Image Analysis* 12 (1), 26–41. doi:10.1016/j.media.2007.06.004.
- Benjamini, Y., Hochberg, Y., 1995. Controlling the false discovery rate: a practical and powerful approach to multiple testing. *J. R. Stat. Soc. Ser. B* 57, 289–300.
- Berryhill, M.E., Phuong, L., Picasso, L., Cabeza, R., Olson, I.R., 2007. Parietal lobe and episodic memory: bilateral damage causes impaired free recall of autobiographical memory. *J. Neurosci.* 27, 14415–14423. doi:10.1523/jneurosci.4163-07.2007.
- Binder, J.R., Desai, R.H., Graves, W.W., Conant, L.L., 2009. Where is the semantic system? A critical review and meta-analysis of 120 functional neuroimaging studies. *Cereb. Cortex* 19, 2767–2796. doi:10.1093/cercor/bhp055.
- Buckner, R.L., Andrews-Hanna, J.R., Schacter, D.L., 2008. The brain's default network: anatomy, function, and relevance to disease. *Ann. N. Y. Acad. Sci.* 1124, 1–38. doi:10.1196/annals.1440.011.
- Burke, J.F., Long, N.M., Zaghoul, K.A., Sharan, A.D., Sperling, M.R., Kahana, M.J., 2014. Human intracranial high-frequency activity maps episodic memory formation in space and time. *NeuroImage* 85, 834–843. doi:10.1016/j.neuroimage.2013.06.067.
- Burke, J.F., Ramayya, A.G., Kahana, M.J., 2015. Human intracranial high-frequency activity during memory processing: neural oscillations or stochastic volatility? *Curr. Opin. Neurobiol.* 31, 104–110. doi:10.1016/j.conb.2014.09.003.
- Burks, J.D., Boettcher, L.B., Conner, A.K., Glenn, C.A., Bonney, P.A., Baker, C.M., Briggs, R.G., Pittman, N.A., O'Donoghue, D.L., Wu, D.H., Sughrue, M.E., 2017. White matter connections of the inferior parietal lobule: a study of surgical anatomy. *Brain Behav.* 7, 1–12. doi:10.1002/brb3.640.
- Cabeza, R., Ciaramelli, E., Olson, I.R., Moscovitch, M., 2008. The parietal cortex and episodic memory: an attentional account. *Nat. Rev. Neurosci.* 9, 613–625. doi:10.1038/nrn2459.
- Caspers, S., Geyer, S., Schleicher, A., Mohlberg, H., Amunts, K., Zilles, K., 2006. The human inferior parietal cortex: cytoarchitectonic parcellation and interindividual variability. *NeuroImage* 33, 430–448. doi:10.1016/j.neuroimage.2006.06.054.
- Conner, C.R., Ellmore, T.M., Pieters, T.A., DiSano, M.A., Tandon, N., 2011. Variability of the relationship between electrophysiology and BOLD-fMRI across cortical regions in humans. *J. Neurosci.* 31, 12855–12865. doi:10.1523/JNEUROSCI.1457-11.2011.
- Corbetta, M., Shulman, G.L., 2002. Control of goal-directed and stimulus-driven attention in the brain. *Nat. Rev. Neurosci.* 3, 201–215. doi:10.1038/nrn755.
- Crone, N.E., Sinai, A., Korzeniewska, A., 2006. High-frequency gamma oscillations and human brain mapping with electrocorticography. *Prog. Brain Res.* 159, 275–295. doi:10.1016/S0079-6123(06)59019-3.
- Daselaar, S.M., Prince, S.E., Cabeza, R., 2004. When less means more: deactivations during encoding that predict subsequent memory. *NeuroImage* 23, 921–927. doi:10.1016/j.neuroimage.2004.07.031.
- Daselaar, S.M., Huijbers, W., Eklund, K., Moscovitch, M., Cabeza, R., 2013. Resting-state functional connectivity of ventral parietal regions associated with attention re-orienting and episodic recollection. *Front. Hum. Neurosci.* 7, 1–9. doi:10.3389/fnhum.2013.00038.
- Desikan, R.S., Ségonne, F., Fischl, B., Quinn, B.T., Dickerson, B.C., Blacker, D., Buckner, R.L., Dale, A.M., Maguire, R.P., Hyman, B.T., Albert, M.S., Killiany, R.J., 2006. An automated labeling system for subdividing the human cerebral cortex on MRI scans into gyral based regions of interest. *NeuroImage* 31, 968–980. doi:10.1016/j.neuroimage.2006.01.021.
- Dickerson, B.C., Miller, S.L., Greve, D.N., Dale, A.M., Albert, M.S., Schacter, D.L., Sperling, R.A., 2007. Prefrontal-hippocampal-fusiform activity during encoding predicts intraindividual differences in free recall ability: an event-related functional-anatomic MRI study. *Hippocampus* 1060–1070. doi:10.1002/hipo.
- Dykstra, A.R., Chan, A.M., Quinn, B.T., Zepeda, R., Keller, C.J., Cormier, J., Madsen, J.R., Eskandar, E.N., Cash, S.S., 2012. Individualized localization and cortical surface-based registration of intracranial electrodes. *NeuroImage* 59, 3563–3570. doi:10.1016/j.neuroimage.2011.11.046.
- Ezzyat, Y., Kragel, J.E., Burke, J.F., Levy, D.F., Lyalenko, A., Wanda, P., O'Sullivan, L., Hurlley, K.B., Busygin, S., Pedisich, I., Sperling, M.R., Worrell, G.A., Kucewicz, M.T., Davis, K.A., Lucas, T.H., Inman, C.S., Lega, B.C., Jobst, B.C., Sheth, S.A., Zaghoul, K., Jutras, M.J., Stein, J.M., Das, S.R., Gorniak, R., Rizzuto, D.S., Kahana, M.J., 2017. Direct brain stimulation modulates encoding states and memory performance in humans. *Curr. Biol.* 27, 1251–1258. doi:10.1016/j.cub.2017.03.028.
- Fellner, M.C., Gollwitzer, S., Rampf, S., Kreiselmeyer, G., Bush, D., Diehl, B., Axmacher, N., Hamer, H., Hanslmayr, S., 2019. Spectral fingerprints or spectral tilt? Evidence for distinct oscillatory signatures of memory formation. *PLoS Biol.* 17, 1–30. doi:10.1371/journal.pbio.3000403.
- Gilmore, A.W., Nelson, S.M., McDermott, K.B., 2015. A parietal memory network revealed by multiple MRI methods. *Trends Cogn. Sci.* 19, 534–543. doi:10.1016/j.tics.2015.07.004.
- Gramfort, A., Luessi, M., Larson, E., Engemann, D.A., Strohmeier, D., Brodbeck, C., Goj, R., Jas, M., Brooks, T., Parkkonen, L., Hämäläinen, M., 2013. MEG and EEG data analysis with MNE-Python. *Front. Neurosci.* 7, 1–13. doi:10.3389/fnins.2013.00267.
- Greenberg, J.A., Burke, J.F., Haque, R., Kahana, M.J., Zaghoul, K.A., 2015. Decreases in theta and increases in high frequency activity underlie associative memory encoding. *NeuroImage* 114, 257–263. doi:10.1016/j.neuroimage.2015.03.077.
- Groppe, D.M., Bickel, S., Dykstra, A.R., Wang, X., Mégevand, P., Mercier, M.R., Lado, F.A., Mehta, A.D., Honey, C.J., 2017. iELVIS: an open source MATLAB toolbox for localizing and visualizing human intracranial electrode data. *J. Neurosci. Methods* 281, 40–48. doi:10.1016/j.neumeth.2017.01.022.
- Hanslmayr, S., Spitzer, B., Bäuml, K.H., 2009. Brain oscillations dissociate between semantic and nonsemantic encoding of episodic memories. *Cereb. Cortex* 19, 1631–1640. doi:10.1093/cercor/bhn197.
- Hanslmayr, S., Volberg, G., Wimber, M., Raabe, M., Greenlee, M.W., Bäuml, K.H.T., 2011. The relationship between brain oscillations and BOLD signal during memory formation: a combined EEG-fMRI study. *J. Neurosci.* 31, 15674–15680. doi:10.1523/JNEUROSCI.3140-11.2011.
- Hanslmayr, S., Staudigl, T., 2014. How brain oscillations form memories – a processing based perspective on oscillatory subsequent memory effects. *NeuroImage* 85, 648–655. doi:10.1016/j.neuroimage.2013.05.121.
- Heinze, S., Sartory, G., Müller, B.W., de Greiff, A., Forsting, M., Jüptner, M., 2006. Neural encoding correlates of high and low verbal memory performance. *J. Psychophysiol.* 20, 68–78. doi:10.1027/0269-8803.20.2.68.
- Herweg, N.A., Solomon, E.A., Kahana, M.J., 2020. Theta oscillations in human memory. *Trends Cogn. Sci.* 24, 208–227. doi:10.1016/j.tics.2019.12.006.
- Hill, P.F., King, D.R., Lega, B.C., Rugg, M.D., 2020. Comparison of fMRI correlates of successful episodic memory encoding in temporal lobe epilepsy patients and healthy controls. *NeuroImage* 207, 116397. doi:10.1016/j.neuroimage.2019.116397.
- Igelström, K.M., Graziano, M.S.A., 2017. The inferior parietal lobule and temporoparietal junction: a network perspective. *Neuropsychologia* 105, 70–83. doi:10.1016/j.neuropsychologia.2017.01.001.
- Kim, H., 2011. Neural activity that predicts subsequent memory and forgetting: a meta-analysis of 74 fMRI studies. *NeuroImage* 54, 2446–2461. doi:10.1016/j.neuroimage.2010.09.045.
- Koen, J.D., Thakral, P.P., Rugg, M.D., 2018. Transcranial magnetic stimulation of the left angular gyrus during encoding does not impair associative memory performance. *Cogn. Neurosci.* 9, 127–138. doi:10.1080/17588928.2018.1484723.
- Lee, H., Chun, M.M., Kuhl, B.A., 2017. Lower parietal encoding activation is associated with sharper information and better memory. *Cereb. Cortex* 27, 2486–2499. doi:10.1093/cercor/bhw097.
- Lindstrom, M.J., Bates, D.M., 1988. Newton-Raphson and EM Algorithms for Linear Mixed-Effects Models for Repeated-Measures Data. *Journal of the American Statistical Association* 83 (404), 1014–1022. doi:10.1080/01621459.1988.10478693.
- Long, N.M., Burke, J.F., Kahana, M.J., 2014. Subsequent memory effect in intracranial and scalp EEG. *NeuroImage* 84, 488–494. doi:10.1016/j.neuroimage.2013.08.052.
- Manning, J.R., Sperling, M.R., Sharan, A., Rosenberg, E.A., Kahana, M.J., 2012. Spontaneously reactivated patterns in frontal and temporal lobe predict semantic clustering during memory search. *J. Neurosci.* 32, 8871–8878. doi:10.1523/JNEUROSCI.5321-11.2012.
- Rugg, M.D., Johnson, J.D., Park, H., Uncapher, M.R., 2008. Chapter 21 Encoding-retrieval overlap in human episodic memory: a functional neuroimaging perspective. *Progress in Brain Research*. Elsevier doi:10.1016/S0079-6123(07)00021-0.
- Rugg, M.D., King, D.R., 2018. Ventral lateral parietal cortex and episodic memory retrieval. *Cortex* 107, 238–250. doi:10.1016/j.cortex.2017.07.012.
- Rutishauser, U., Afkhal, T., Rosario, E.R., Pouratian, N., Andersen, R.A., 2018. Single-neuron representation of memory strength and recognition confidence in left human posterior parietal cortex. *Neuron* 97, 209–220. doi:10.1016/j.neuron.2017.11.029.
- Seabold, S., Perktold, J., 2010. Statsmodels: econometric and statistical modeling with python. In: *Proceedings of the 9th Python in Science Conference*, pp. 92–96.
- Serruya, M.D., Sederberg, P.B., Kahana, M.J., 2014. Power shifts track serial position and modulate encoding in human episodic memory. *Cereb. Cortex* 24, 403–413. doi:10.1093/cercor/bhs318.
- Sestieri, C., Capotosto, P., Tononi, A., Luca Romani, G., Corbetta, M., 2013. Interference with episodic memory retrieval following transcranial stimulation of the inferior but not the superior parietal lobule. *Neuropsychologia* 51, 900–906. doi:10.1016/j.neuropsychologia.2013.01.023.
- Sestieri, C., Shulman, G.L., Corbetta, M., 2017. The contribution of the human posterior parietal cortex to episodic memory. *Nat. Rev. Neurosci.* 18, 183–192. doi:10.1038/nrn.2017.6.
- Shrager, Y., Kirwan, C.B., Squire, L.R., 2008. Activity in both hippocampus and perirhinal cortex predicts the memory strength of subsequently remembered information. *Neuron* 59, 547–553. doi:10.1016/j.neuron.2008.07.022.
- Solomon, E.A., Stein, J.M., Das, S., Gorniak, R., Sperling, M.R., Worrell, G., Inman, C.S., Tan, R.J., Jobst, B.C., Rizzuto, D.S., Kahana, M.J., 2019. Dynamic theta networks in the human medial temporal lobe support episodic memory. *Curr. Biol.* 29, 1100–1111. doi:10.1016/j.cub.2019.02.020.
- Staresina, B.P., Davachi, L., 2006. Differential encoding mechanisms for subsequent associative recognition and free recall. *J. Neurosci.* 26, 9162–9172. doi:10.1523/JNEUROSCI.2877-06.2006.
- Uncapher, M.R., Wagner, A.D., 2009. Posterior parietal cortex and episodic encoding: insights from fMRI subsequent memory effects and dual-attention theory. *Neurobiol. Learn. Mem.* 91, 139–154. doi:10.1016/j.nlm.2008.10.011.
- Vilberg, K.L., Rugg, M.D., 2008. Memory retrieval and the parietal cortex: a review of evidence from a dual-process perspective. *Neuropsychologia* 46, 1787–1799. doi:10.1016/j.neuropsychologia.2008.01.004.
- Wagner, A.D., Shannon, B.J., Kahn, I., Buckner, R.L., 2005. Parietal lobe contributions to episodic memory retrieval. *Trends Cogn. Sci.* 9, 445–453. doi:10.1016/j.tics.2005.07.001.
- Winawer, J., Kay, K.N., Foster, B.L., Rauschecker, A.M., Parvizi, J., Wandell, B.A., 2013. Asynchronous broadband signals are the principal source of the bold response in human visual cortex. *Curr. Biol.* 23, 1145–1153. doi:10.1016/j.cub.2013.05.001.
- Xia, M., Wang, J., He, Y., 2013. BrainNet viewer: a network visualization tool for human brain connectomics. *PLoS One* 8. doi:10.1371/journal.pone.0068910.
- Yeo, B.T.T., Krienen, F.M., Sepulcre, J., Sabuncu, M.R., Lashkari, D., Hollinshead, M., Roffman, J.L., Smoller, J.W., Zöllei, L., Polimeni, J.R., Fisch, B., Liu, H., Buckner, R.L., 2011. The organization of the human cerebral cortex estimated by intrinsic functional connectivity. *J. Neurophysiol.* 106, 1125–1165. doi:10.1152/jn.00338.2011.